STUDY OF OPTICAL ENERGY GAP AND QUANTUM CONFINMENT EFFECTS IN ZINC OXIDE NANOPARTICLES AND NANORODS

I. MUSA*, N. QAMHIEH
[a]*Department of Physics, Palestine Technical University-Kadoorie, Tulkarm, P.O. Box 7, Palestine*
[b]*Department of Physics, UAE University, Al-Ain, P.O. Box 15551, United Arab Emirates*

ZnO sol-gel nanoparticles (NPs) and nanorods (NRs) were prepared by simple chemical method. The resulting NPs and NRs have been characterized by X-Ray Diffraction, TEM, UV-Vis absorption and steady-state photoluminescence (PL) spectroscopy.(XRD) results showed that all samples were single phase wurtzite structure and broadening peaks for ZnO nanoparticles as compared to NRs. The morphology of the nanostructures was observed in transmission emission microscope. The NPs have average diameter ~ 4 nm and the NRs have ~ 18 nm diameter and ~ 100 nm length. The band gap was calculated from the UV-Visible spectrum and found to be 3.39 eV for NPs and 3.2 eV for NRs. This variation of optical energy gap is due to quantum confinement effect when is the material changed from nanoparticles to nanorods. However, the measured NPs and NRs diameters indicate that the charge carriers are located in a strong and weak confinement regime, respectively.The PL reveals that the ultraviolet emission intensity of ZnO nanoparticles decreases from 396 to 367 nm and shifts towards the blue region by reducing the size as compared to nanorods which is consistent with UV-visible absorption.

(Received October 16, 2018; Accepted February 14, 2019)

Keywords: Nanoparticles, Nanorods, Optical band gap, Steady-state photoluminescence

1. Introduction

Wurzite zinc oxide (ZnO) is a well-known semiconductor material, with research going back to the first quarter of the last century [1]. It belongs to the group of II-VI compound with a direct- wide bandgap (WBG)semiconductor (E_g~ 3.37 eV) at room temperature [2]. In the last decade, research interest in ZnO nanostructure was regenerated because of the processing method used to fabricate ZnO lead to different properties. It attracted great attention in research due to its unique properties and versatile application in biomedical [3], piezoelectronic devices, transparent electronics, and chemical sensors [4,5]. Also, ZnO possesses high exciton binding energy of (60 meV) at room temperature which makes it promising in applications like optoelectronic devices [6,7]. Furthermore, ZnO has a large number of extrinsic and intrinsic deep-level impurities that emit light of different colors, including violet, blue, green, yellow, orange and red [8,9]. Another area of interest is based on the length scale of the ZnO nanostructure. When the size of semiconducting-nanostructuers is reduced to the order of Bohr radius of bulk exciton(few nanometers), quantum confinement effect occurs and the optical properties of exciton are changed. This effect was observed by Berry [10,11]and Brus [12] for reduced size nanocrystals in a colloidal dispersion. The quantum confinement can be related to the increase of the band gap when the particle size decreases, which causes a blue shift of the emission as a result of bandgap widening. The quantum confinement depends on the ratio of the nanostructuers radius to Bohr exciton radius of the bulk. It can be classified to weak, intermediate and strong confinement regimes [13,14].

* Corresponding author: i.musa@ptuk.edu.ps

In this paper, we have studied the variation of the energy gap and emission characteristics of nanoparticles and nanorods. The existence of confinement effect in ZnO nanoparticles and nanorods has been revealed by comparing the peak positions of exciton emissions with the nanoparticles and nanorods sizes.

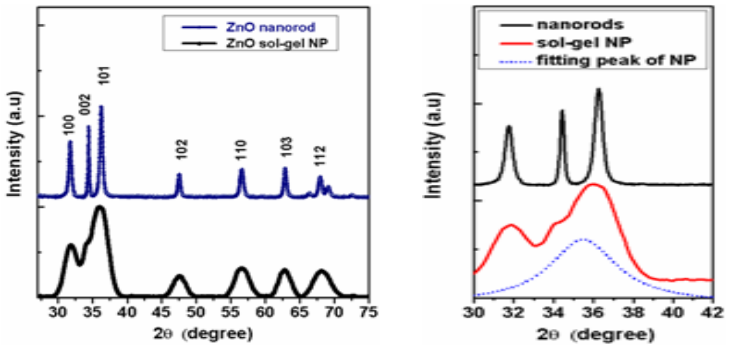

Fig. 1. X-ray diffraction pattern of ZnO nanostructuers (a) between 30° and 70° and (b) enlarged view from 30° to 42°.

2. Experimental methods

Synthesized ZnO sol-gel nanoparticles and nanorods were reported in previous work [15]. Briefly, a 5.5 g of zinc acetate dehydrate (98+%, sigma Aldrich) in 250 ml of ethanol was heated until the solution became clear. This solution was refluxed for 1hr, and 150 ml of the solvent was removed by distillation and replaced by the same amount of fresh ethanol. After that, 1.39 g of lithium hydroxide monohydrate (Aldrich) was added to the solution in an ultrasonic bath at 0 ℃. The mixture was dispersed for 1h to obtain a transparent solution consisting of ZnO sol-gel nanoparticles. The solution was filtered through a 0.1 μm membrane filter to remove undissolved LiOH. To get ZnO nanorods product, the solution of 100 ml containing ZnO nanoparticles was heated and mixed with 10% of distilled water (DW) at 60 ℃ for 18 hours. During this process, a white powder-precipitate was formed. Then the solution was centrifuged and washed four times with ethanol–water mixture (19:1) to remove physisorbedionic compounds.

Powder X-ray diffraction (XRD) patterns were obtained at room temperature using Shimadzu 6100 XRD and CuKα radiation (λ= 0.15406 nm).The morphology of ZnO nanoparticles and nanorods were analyzed using transmission electron microscope (TEM) using Tecnai G2 F20 Spirit BioTwin, Netherlands. The optical absorption spectra were obtained using Jasco UV–Visible spectrophotometer. Steady-state photoluminescence measurements were carried out by Varian Cary Eclipse Fluorescence Spectrophotometer with excitation wavelength of 320 nm.

3. Results and discussion

X-ray diffraction measurements were performed on thin films of sol-gel nanoparticles deposited on glass substrateat room temperature and ZnO nanorods powder. The resulted X-ray diffraction patterns are shown in Fig.1.The diffraction peaks in the patterns can be attributed to the presence of hexagonal wurzite crystallites. Also, it is clear that no excess peaks are observed, which indicates that no complex product was formed. It is worth noting that the full width at have maximum (FWHM) of the diffraction peaks for ZnO nanoparticles are more broadening than nanorods. It can be attributed to the small sizes of nanoparticles. The FWHM of the peak (101) in the XRD pattern is used for determining the average crystallite size using equation 1; the Debye-Scherer formula [16]:

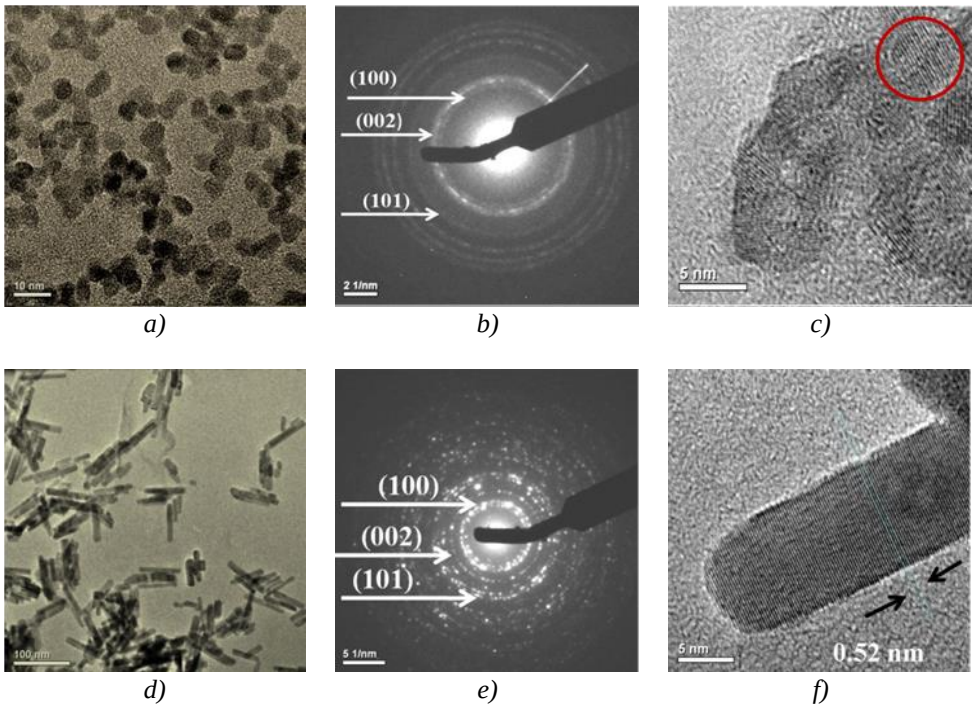

Fig.1. TEM images of ZnO nanostructures. (a) HRTEM of sol-gel nanoparticles disperse in ethanol, (b) corresponding selected area electron diffraction (SAED) of sol-gel NP, (c) image of individual nanoparticles (Lattice image),(d)HRTEM of nanorods disperse in ethanol, (e) corresponding selected area electron diffraction (SAED) of nanorods, (f) image of individual nanorods (Lattice image).

$$Average\ crystallite\ size\ (D) = \frac{0.9\lambda}{\beta cos\theta} \tag{1}$$

where d is the average size of the particles, λ is the wavelength of X-ray = 0.15406 nm, β is the angular peak width at half-maximum in radian along (101) plane and θ is Bragg's diffraction angle. The micro-strain (ε) can be calculated using the formula [17]:

$$micro - strain\ (\varepsilon) = \frac{\beta cos\theta}{4} \tag{2}$$

Table 1 shows the results of full width at half-maximum (FWHM), average crystallite size (D) and micro-strain (ε) of ZnO nanoparticles and nanorods.The calculated average crystallite size of ZnO nanoparticles is about ~ 4 nm and ~ 18.2 nm for nanorods.The micro-strain (ε) that influences the peak broadening of sol-gel nanoparticles is due to contributions from lattice defects. Also, it is clear that the strain in the ZnO nanostructures is inversely proportional to the crystallite size as reported in the literature [18]. Fig. 2(a) shows the TEM images of sol-gel ZnO NP dispersed in ethanol. The size of isolated nanoparticles is about 4–5 nm that is close to the X-ray diffraction calculation. The selected area electron diffraction (SAED) of ZnO NP is shown in Fig. 2(b). The diffraction rings indicates that the synthesized nanoparticles have a polycrystalline nature of ZnO. These diffraction rings are due to reflections from (1 0 0) (0 0 2) (1 0 1) planes. Fig. 2(c) shows the Lattice image of individual nanoparticles which is structurally uniform and well- oriented lattice fringe of d-spacing.

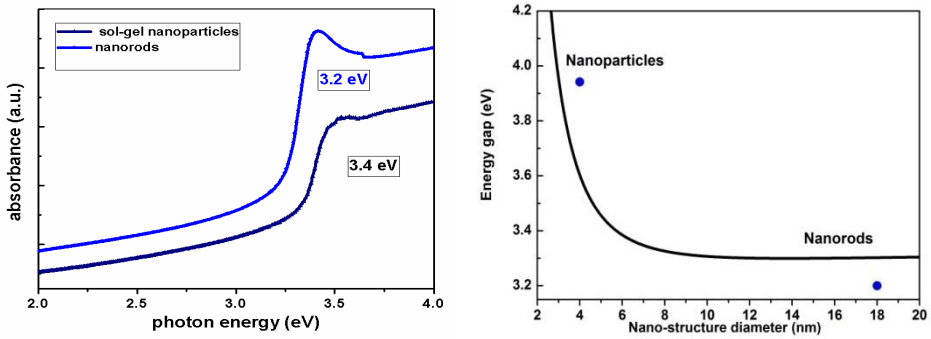

a) *b)*

Fig.2. (a). Room temperature UV–Visible absorption spectra near the band edge as a function of photon enegy (eV) of ZnO sol-gel nanoparticles and nanorods. (b) Dependence of the lowest excited state vs ZnO nanostructures diameter (solid line).Circles correspond to the optical absorption onsets determined experimentally.

Fig. 2 (e) shows the TEM images of ZnO NRs powder dispersed in ethanol. The size of single ZnO NR is about ~ 18 nm and length ~ 100 nm. A Corresponding selected area electron diffraction (SAED) pattern of local crystal structure is shown in Fig. 2 (e). The diffraction rings indicates that the synthesized nanorods are polycrystalline in nature. These diffraction rings are from (1 0 0) (0 0 2) (1 0 1) planes. Moreover, the bright spots appear on the polycrystalline diffraction rings indicate the presence of well crystalline ZnO NRs. The HR-TEM images of individual ZnO NR are presented in Fig. 2 (f).The lattice distance is estimated 0.52 nm, which is consistent with the distance of (001) planes of ZnO wurtzite hexagonal structure.

In order to investigate the band gap variation related to the quantum confinement effects, optical absorption for ZnO nanoparticles and nanorods have been obtained. The absorption data at room temperature for ZnO nanostrucuers are shown in Fig. 3 (a). From this figure, it can be observed that the excitonic peak/absorption band edge is found to be blue shifted from 3.2 to 3.4eV as the nanostructures change from nanorods to nanoparticle sizes.The optical band gaps of the ZnO nanostructures (NPs and NRs) were calculated using Tauc equation [19]:

$$(\alpha h\nu)^{1/n} = A(h\nu - E_g), \tag{3}$$

Here, $h\nu$ is the energy of the incident photon, αA is the absorption coefficient, E_g is the optical band gap energy and the exponent n depends of the type of transition between bands. Since adirect transition is considered for ZnO, $n = 1/2$for our estimations.The plot of $(\alpha h\nu)^2$ versus ($h\nu$) is shown in Fig. 4. By extrapolating the linear portion of the plot, thex-axis intercept indicates the band gap value for ZnO NPs and NRs were estimated to be ~ 3.39 eV and 3.2 eV, respectively.The blue shift can be attributed to the optical confinement effect correspond to the small size of ZnO nanostructures (NPs and NRs) [20].

Table 1: Full width half-maximum (β), average crystallite size (D) and micro-strain (ε) of ZnO nanoparticles and nanorods

Type ofnanostructuers	FWHM, β (deg)	Average crystallite size, D (nm)	micro − strain (ε)10^{-4}
ZnO nanoparticles	2.9	4	120
ZnOnanorods	0.46	18.2	19

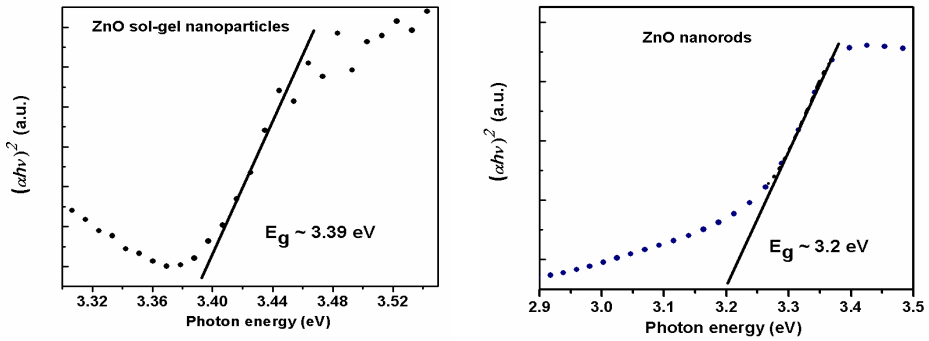

Fig. 3.Tauc plot from UV–Vis analysis of a ZnO, (a) nanoparticles and (b) nanorods that illustrates the fitting of the linear region to evaluate the optical band-gap at the X-axis intercept.

Fig. 3 (b) shows the optical absorption depicting the energy of the lowest excited state of the exciton shifts towards high energies as the size of nanostructure change from NRs to NPs. This trend can be reproduced theoretically by expressing the energy of the lowest excited state as a function of the nanostructures size (radius) by the following equation [21]:

$$E = E_g + \frac{\pi^2 \hbar^2}{2R^2 \mu_{e,h}} - \frac{1.786 e^2}{4\pi\varepsilon_0 \varepsilon R}\ , \tag{4}$$

where $\boldsymbol{\varepsilon_0}$ and $\boldsymbol{\varepsilon}$ are the permittivity of free space and for particles, **e** the elementary charge, and $\boldsymbol{\mu_{e,h}}$ the reduced effective mass of the electron (m_e^*) and the hole (m_e^*). The best fit for Eq. (4) to the experimental absorption mid-edge energies is obtained by taking $m_e^* = 0.24$, $m_h^* = 0.45$ and $\varepsilon = 3.7$, in good agreement with the quantum confinement model. We expect that the nanoparticles with size radiusof 4 nm smaller than the bulk ZnO Bohr radius($a_B = 2.34\, nm$) [22] can relatively have high exciton energy, and that the charge carriers are presented in astrong confinement regime.Exciton energy in nanorods with radius larger than the ZnO Bohr radius is relatively larger, and carriers in this nanorod should lie in aweak quantum confinement regime [23].The energy of the lowest excited state will be saturated while extending to the upper size limit of 18 nm.

Since the quantum confinement affects the electronic band structure of the semiconductors materials, it is expected that for small sizes of nanostructures, the photoluminescence properties will be different. The PL properties of different types ZnO nanostructures demonstrated a relative intensity emission between the UV- visible emission and the point defects such as oxygen deficiency in the crystalline structure of the material. This relative intensity can be observed on PL measurements. Fig. 5 (a) and (b) shows the room temperature PL emission spectra of ZnO nanostructures (sol-gel NPs and powder NRs). Both samples show a strong and narrow UVemission peak around 368 nm (3.7 eV) for NPs and 397 (3.1 eV) nm for NRs, which is identified as the near band-edge (NBE) emission of the free exciton [24]. Also, a broad emission band in the visible region of the spectrum in the wavelength range 450–650 nm is observed, which is generally attributed to deep level defects, such as oxygen vacancies and interstitials of zinc and oxygen [25,26]. Green luminescence photograph digit of ZnO sol- gel nanoparticles under irradiation by 365 nm ultraviolet light are presented in fig. 5 (c). It is clear that the green luminescence arises from defects in ZnO(sol-gel NPs) are dominated. It is worth noting that the relative intensity of two bands depends on the type of ZnO nanostructures. The broad band at around 450-650 nm centered at 520 nm for NPs is enhanced. It can be attributed by increasing the total surface area in the particles ensemble volume resulting from the decrease of the individual particles surface and larger surface area to volume ratio [27]. Moreover, Fig. 5 (d) shows the blue shift of the UV peak from 396 to 368 nm with change from nanorods to nanoparticles. The blue shift behavior is naturally explained by the expected quantum confinement, which generally shifts the energy levels of the conduction and valence bands apart, causing a blue shift in the transition

energy as the size of nanostructures decreases. The PL results are in good agreement with optical energy gap study shown in Fig. 4.

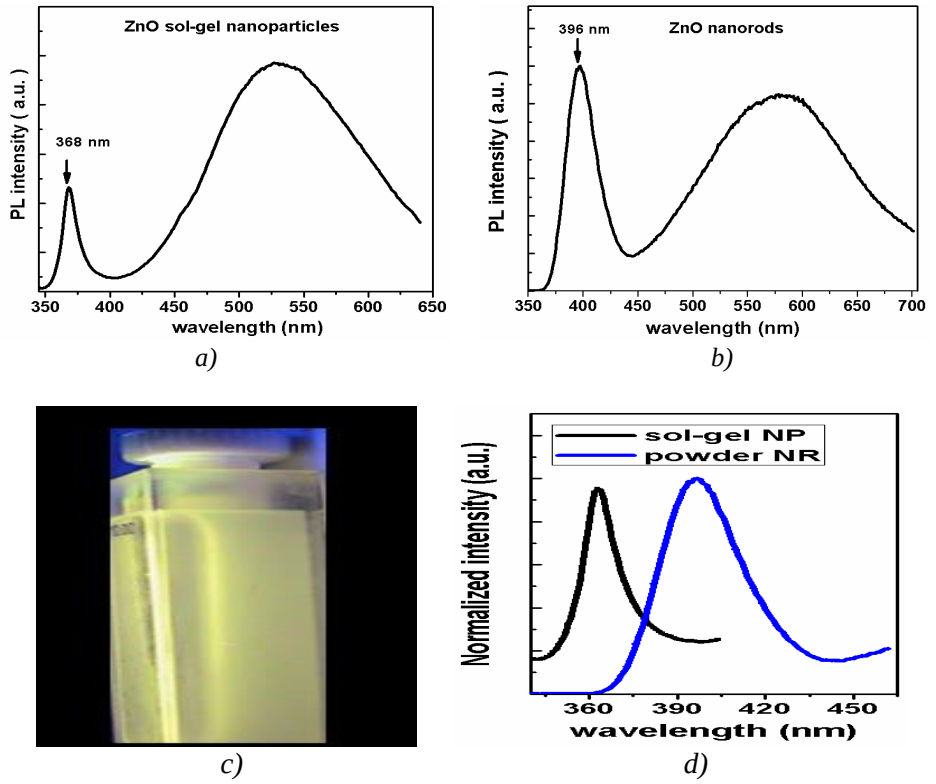

Fig.4. Room temperature steady state PL emission spectra of ZnO nanostructures (a) sol-gel nanoparticles, (b) nanorods, (c) Green luminescence photograph digit of ZnO sol- gel nanoparticles under irradiation with 365 nm ultraviolet light from a UV lamp, and (d) the blue shift of the UV peaks.

4. Conclusions

In conclusion, the variations of optical energy gap for ZnO nanostructures (NPs and NRs) have been studied. The nanoparticles and nanorods exhibit strong absorption at ~ 3.4, and 3.2 eV respectively. The ZnO NPs and NRs have band gap variation from 3.2 eV to 3.39 eV, as calculated from the absorption data, by reducing the size of nanostructures. This band gap enhancement occurs due to quantum confinement effect of exciton within the small dimension of the nanostructures. Also the study shows that the NPs lie in a strong regime, while the NRs in a weak confinement regime.The PL intensity reveals that the ultraviolet emission intensity of ZnO nanoparticles decreases from 396 to 367 nm and shift towards blue region as the size reduced from that for nanoparticles to that of nanorods.

Acknowledgment

The authors are thankful for the financial support from the Palestinian Ministry of Higher Education and PTUK.

References

[1] C. Klingshirn, J. Fallert, H. Zhou, J. Sartor, C. Thiele, F. Maier-Flaig, D. Schneider, H. Kalt, Physica Status Solidi (B) **247**, 1424 (2010).
[2] Ü. Özgür, Y. I. Alivov, C. Liu, A. Teke, M. A. Reshchikov, S. Doğan, V. Avrutin, S.-J. Cho, H. Morkoç, Journal of Applied Physics **98**, 041301 (2005).
[3] Y. Zhang, T. R. Nayak, H. Hong, W. Cai, Curr Mol Med **13**, 1633 (2013).
[4] D. Calestani, M. Zha, R. Mosca, A. Zappettini, M. C. Carotta, V. Di Natale, L. Zanotti, Sensors and Actuators B: Chemical **144**, 472 (2010).
[5] J. Zhou, Y. Gu, P. Fei, W. Mai, Y. Gao, R. Yang, G. Bao, and Z. L. Wang, Nano Lett. 8, 3035 (2008).
[6] R. V. Hariwal, H. K. Malik, A. Negi, A. Kandasami, RSC Advances **8**, 6278 (2018).
[7] M. Y. Zhou, L. S. Qu, H. Gao, IOP Conference Series: Materials Science and Engineering **213**, 012009 (2017).
[8] M. Willander, O. Nur, Q. X. Zhao, L. L. Yang, M. Lorenz, B. Q. Cao, J. Zúñiga Pérez, C. Czekalla, G. Zimmermann, M. Grundmann, A. Bakin, A. Behrends, M. Al-Suleiman, A. El-Shaer, A. Che Mofor, B. Postels, A. Waag, N. Boukos, A. Travlos, H. S. Kwack, J. Guinard, D. Le Si Dang, Nanotechnology **20**, 332001 (2009).
[9] W. Liu, S. L. Gu, J. D. Ye, S. M. Zhu, S. M. Liu, X. Zhou, R. Zhang, Y. Shi, Y. D. Zheng, Y. Hang, C. L. Zhang, Appl. Phys. Lett. **88**, 092101 (2006).
[10] C. R. Berry, Phys. Rev. **153**, 989 (1967).
[11] C. R. Berry, Phys. Rev. **161**, 848 (1967).
[12] L. Brus, The Journal of Physical Chemistry **90**, 2555 (1986).
[13] L. Irimpan, V. P. N. Nampoori, and P. Radhakrishnan, J. Appl. Phys. **104**, 113112 (2008).
[14] N. Janβen, K. M. Whitaker, D. R. Gamelin, R. Bratschitsch, Nano Letters **8**, 1991 (2008).
[15] I. Musa, N. Qamhieh, S. T. Mahmoud, Results in Physics **7**, 3552 (2017).
[16] J. C. Nie, J. Y. Yang, Y. Piao, H. Li, Y. Sun, Q. M. Xue, C. M. Xiong, R. F. Dou, Q. Y. Tu, Appl. Phys. Lett. **93**, 173104 (2008).
[17] M. S. Geetha, H. Nagabhushana, H. N. Shivananjaiah, Journal of Science: Advanced Materials and Devices **1**, 301 (2016).
[18] V. Koutu, L. Shastri, M. M. Malik, Materials Science-Poland **34**, 819 (2016).
[19] B. D. Viezbicke, S. Patel, B. E. Davis, D. P. Birnie, Physica Status Solidi (B) **252**, 1700 (2015).
[20] K. Foo, U. Hashim, K. Muhammad, C. Voon, Nanoscale Research Letters **9**, 429 (2014).
[21] L. E. Brus, The Journal of Chemical Physics **80**, 4403 (1984).
[22] R. T. Senger, K. K. Bajaj, Physical Review B **68**, (2003).
[23] I. Musa, F. Massuyeau, L. Cario, J. L. Duvail, S. Jobic, P. Deniard, E. Faulques, Applied Physics Letters **99**, 243107 (2011).
[24] A. Sasaki, W. Hara, A. Matsuda, N. Tateda, S. Otaka, S. Akiba, K. Saito, T. Yodo, M. Yoshimoto, Appl. Phys. Lett. **86**, 231911 (2005).
[25] Z. Zhang, H. Xiong, Materials **8**, 3101 (2015).
[26] M. D. McCluskey, S. J. Jokela, J. Appl. Phys. **106**, 071101 (2009).
[27] K. Suzuki, H. Kondo, M. Inoguchi, N. Tanaka, K. Kageyama, H. Takagi, Appl. Phys. Lett. **94**, 223103 (2009).